Supporting Information

A facile hydrothermal method to synthesize $Sb_2S_3/Sb_4O_5Cl_2$ composite with three-dimensional spherical structure

Qian Jiang [a, b], Xingzhong Yuan [a, b *], Hou Wang [a, b], Xiaohong Chen [c], Shansi Gu [a, b], Yang Liu [a, b], Zhibin Wu [a, b], Guangming Zeng [a, b]

[a] College of Environmental Science and Engineering, Hunan University, Changsha 410082, PR China

[b] Key Laboratory of Environment Biology and Pollution Control, Hunan University, Ministry of Education, Changsha 410082, PR China

[c] Collaborative Innovation Center of Resource-Conserving & Environment-Friendly Society and Ecological Civilization, Changsha 410083, PR China

[*] Corresponding author at: College of Environmental Science and Engineering, Hunan University, Changsha 410082, PR China. Tel.: +86 731 88821413; fax: +86 731 88823701.
E-mail address: yxz@hnu.edu.cn (X.Z. Yuan)

Experimental Section

Preparation: All the reactants and solvents were of analytical grade and used without further purification. To synthesize $Sb_2S_3/Sb_4O_5Cl_2$, some procedures were carried out: primarily, 2.282 g $SbCl_3$ was dissolved into 20.0 mL HCl (6 mol/L) solution to form a homogeneous mixture solution. Subsequently, the mixture solution was added into 50.0 ml NaOH (2 mol/L) solution and stirring for 30 min at room temperature. Different mass of Na_2S in 15 mL distilled water was added dropwise into the previous solution under stirring for 10 min at room temperature. Next, the resulting mixture was transferred into 100 mL Teflon-lined steel autoclaves, maintained at 100 °C for 12 h and followed by cooling naturally to room temperature. Finally, the products were filtered, washed several times by water and then dried under vacuum at 60 °C. A series of $Sb_2S_3/Sb_4O_5Cl_2$ composites were prepared by changing the amount of Na_2S. For comparison, pure $Sb_4O_5Cl_2$ was prepared without Na_2S under the same conditions.

Characterization: The X-ray diffraction (XRD) patterns were recorded on Bruker AXS D8 Advance diffractometer using Cu-Ka source (λ = 1.541 Å) with the range of the diffraction angle of (2θ) 15–75°. The surface elemental composition analyses were conducted based on the X-ray Photoelectron Spectroscopy spectra (XPS) (Thermo Fisher Scientific, UK). The morphology of the samples was studied by a field emission scanning electron microscopy (FESEM) (JSM-7001F, Japan) and electrion microscopy TM3000. High-resolution transmission electron microscopy (HRTEM) images were obtained by using a Hitachi H 600 electron microscope (Japan) with an accelerating voltage of 100 kV. Ultravioletvisible (UV-vis) detection was carried out on a Varian Cary 300 spectrometer outfitted with an integrating sphere.

Photocatalytic Activity Measurements: The photocatalytic activity of the as-prepared samples was evaluated by photodegradation of MO aqueous solution under visible light. The visible-light source used in the measurements was a 500 W Xe lamp (Beijing China Education Au-light Co. Ltd) irradiation with a 420 nm cut-off filter. Typically, 100 mg powdered samples were dispersed into 100 mL of 15 mg/L MO solution. In order to attain adsorption- desorption equilibrium, the suspension was stirred for 1 h in the dark prior to irradiation. At given time intervals, 4 mL of the mixture was withdrawn from the reaction system and centrifuged at 9000 rpm for 5 min to remove the suspended catalyst particles. The residual MO concentration was measured using a UV–vis spectrophotometer (UV-2250, SHIMADZU Corporation, Japan) at the wavelength of 463 nm.

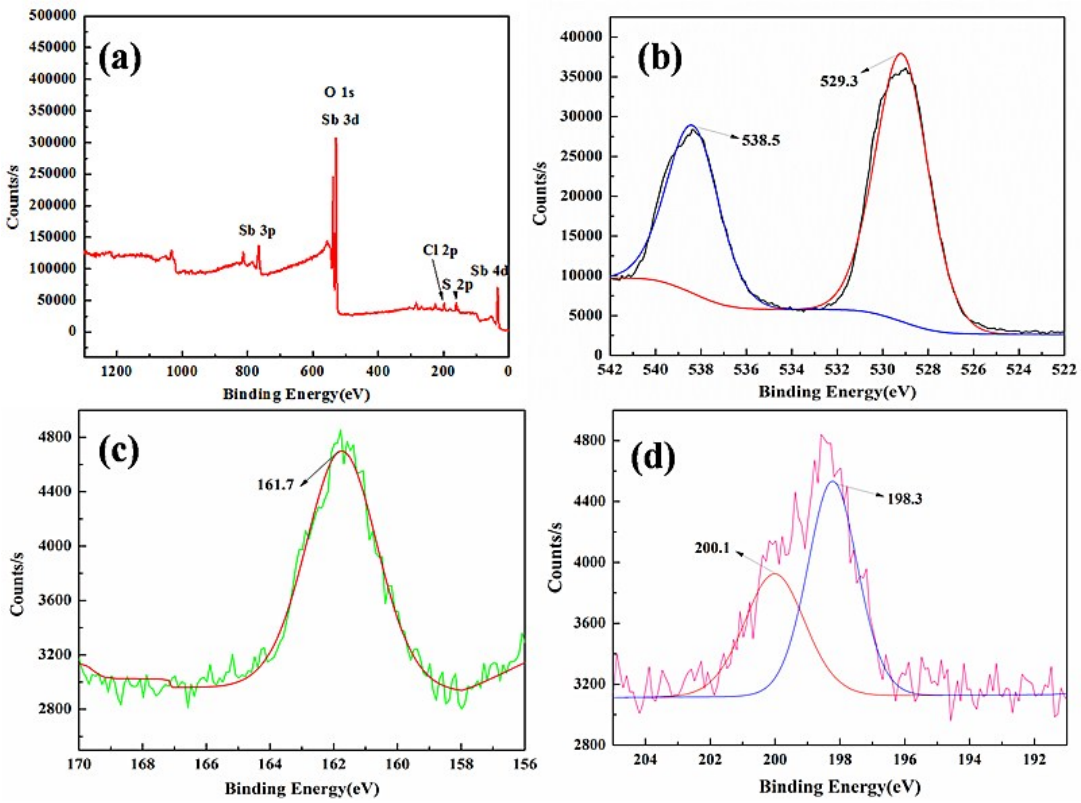

Fig.S1. XPS spectra of C2: (a) survey spectrum, (b) Sb 3d, (c)S 2p, (d) Cl 2p.

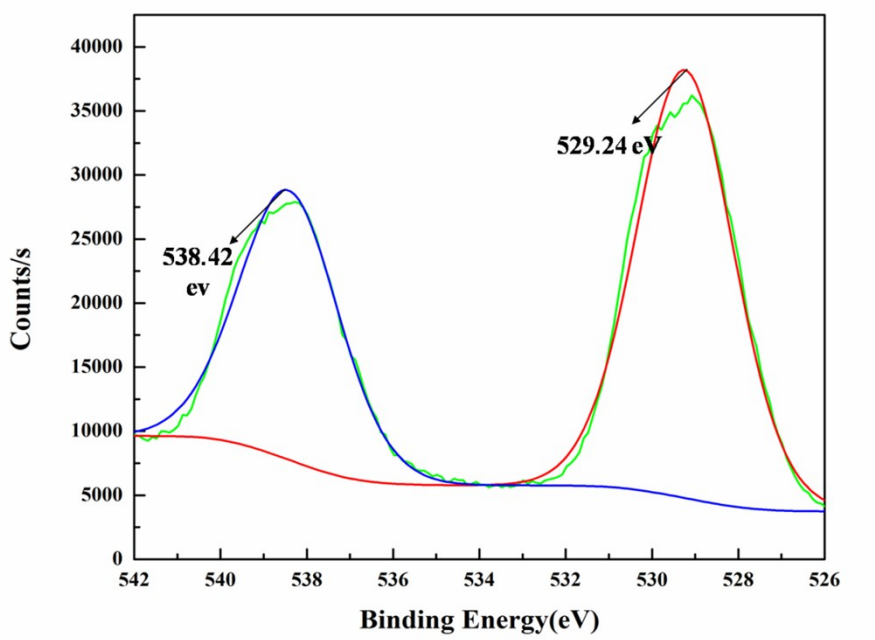

Fig.S2. XPS spectra of C2: O 1s.

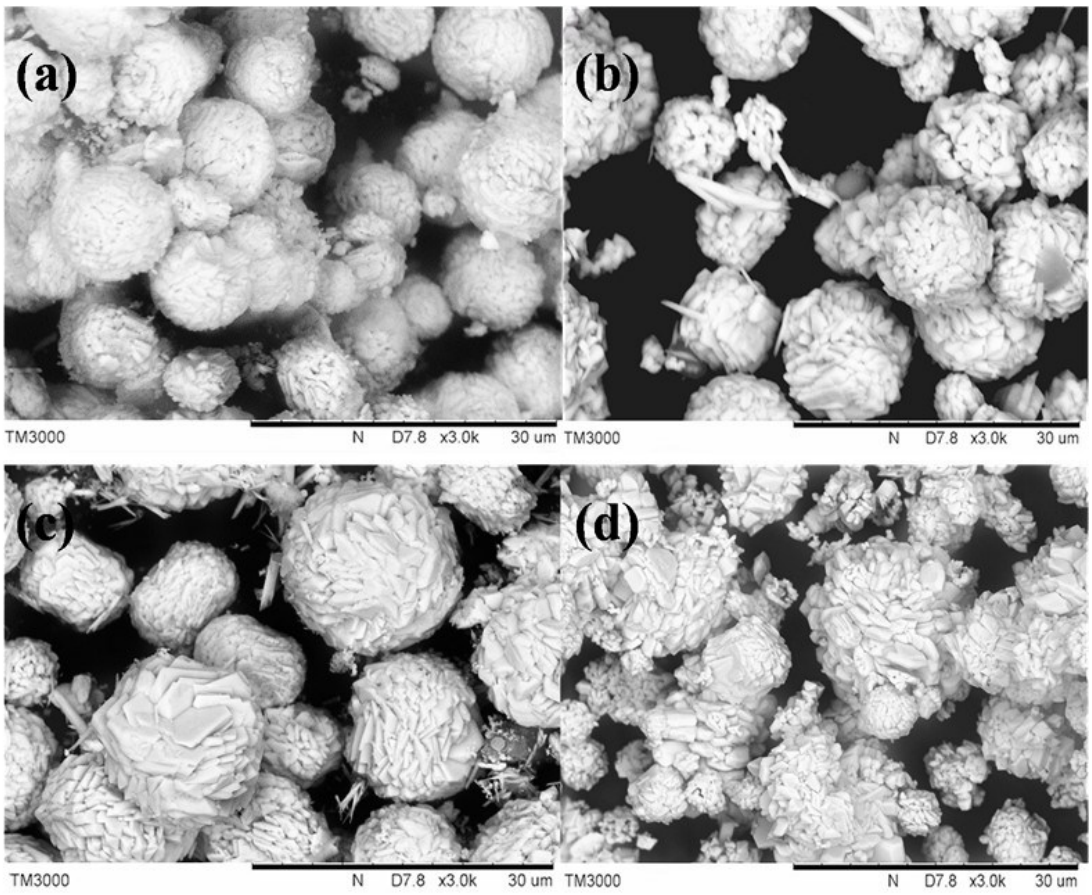

Fig.S3. SEM images of (a) C1, (b) C2, (c) C3 and (d) $Sb_4O_5Cl_2$;

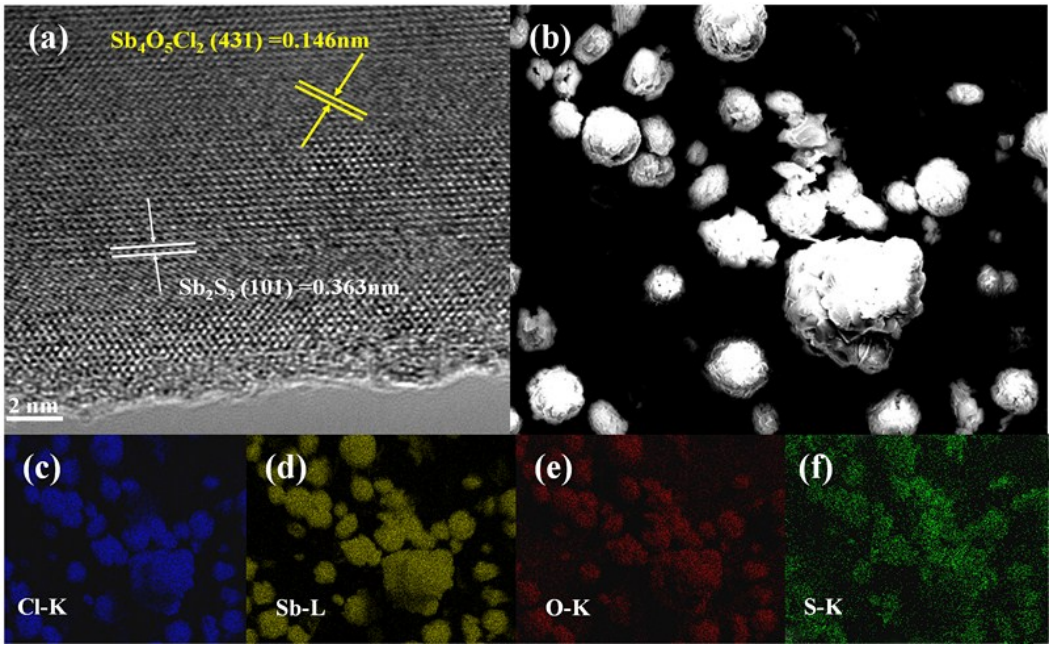

Fig.S4. (a) HRTEM image of C2, (b-f) Elemental mapping images of C2.

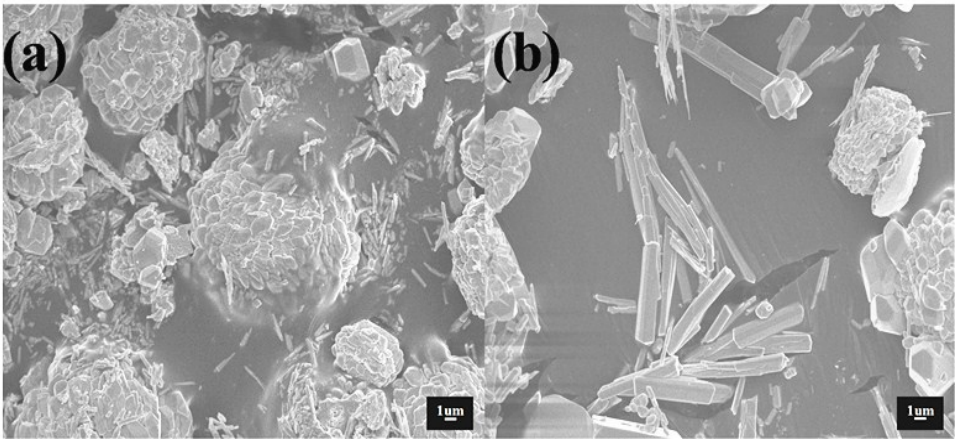

Fig.S5. SEM images of the as-synthesized samples with different reaction temperature: (a) 150°C; (b) 200°C.

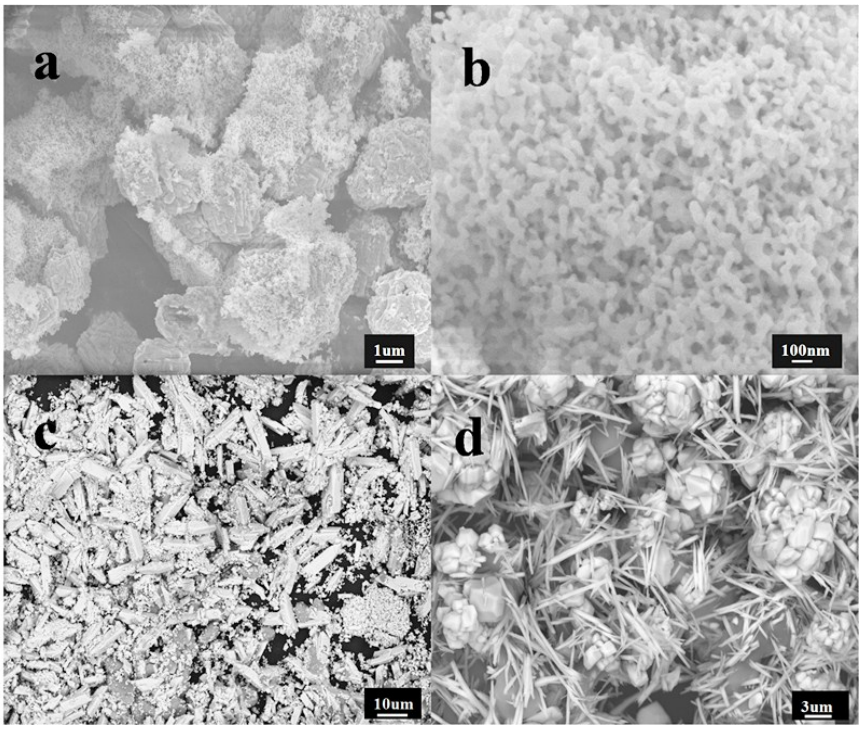

Fig.S6. (a), (b) SEM images of the samples before hydrothermal reaction; (c) SEM images of the $Sb_2S_3/Sb_4O_5Cl_2$ prepared in another HCl concentration without adding NaOH; (d) SEM images of the $Sb_2S_3/Sb_4O_5Cl_2$ prepared in the same HCl concentration without adding NaOH.

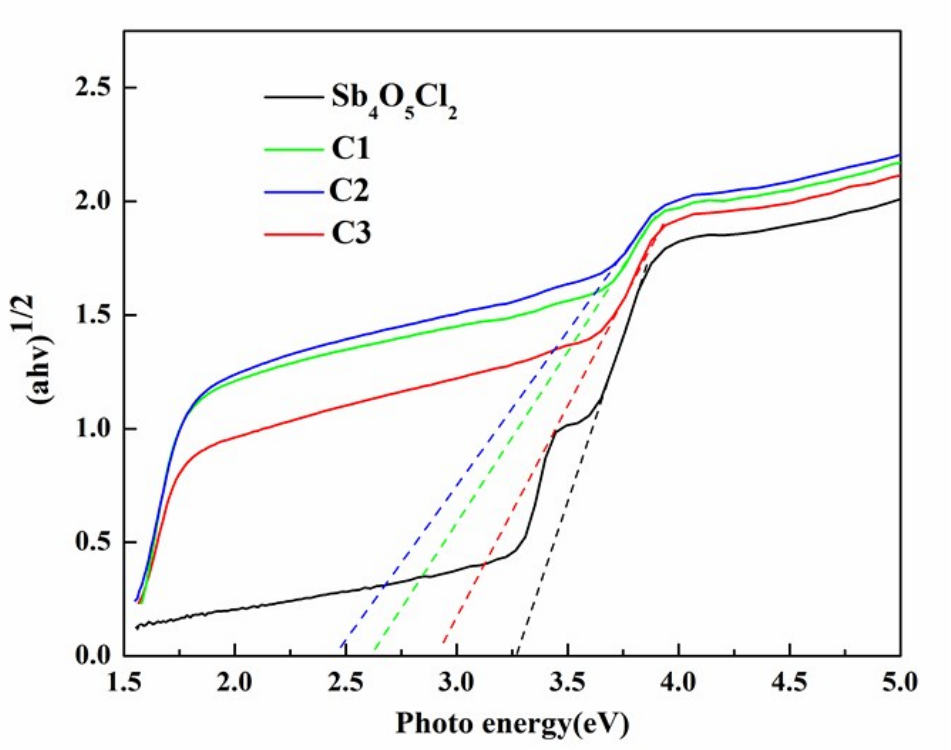

Fig.S7. the band gaps (Eg) of different samples.

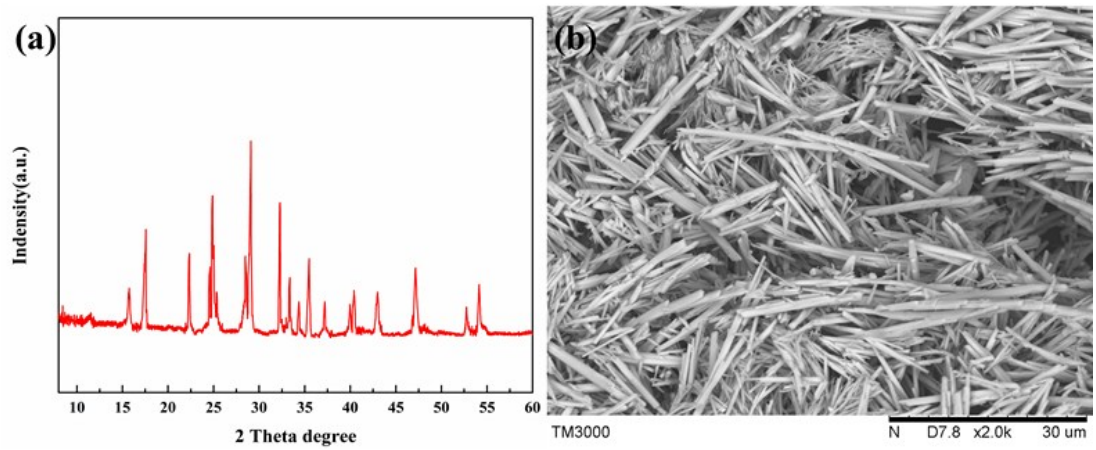

Fig. S8. (a) XRD pattern of the as-prepared pure Sb_2S_3, (b) SEM image of the as-prepared pure Sb_2S_3.

Preparation of pure Sb_2S_3: 2.282 g $SbCl_3$ was dissolved into 20.0 mL HCl (6 mol/L) solution to form a homogeneous mixture solution A, 3.6 g of sodium sulfide ($Na_2S.9H_2O$) was dissolved in 50.0 ml NaOH (2 mol/L) solution to obtain solution B. Subsequently, the mixture solution A was added into the solution B (the method could avoid $SbCl_3$ hydrolyzing to produce $Sb_4O_5Cl_2$), and stirring for 30 min at room temperature. Next, the resulting mixture was transferred into 100 mL Teflon-lined steel autoclaves, maintained at 100 °C for 12 h and followed by cooling naturally to room temperature. Finally, the products were filtered, washed several times by water and then dried under vacuum at 60 °C.

The XRD pattern of the as-prepared pure Sb_2S_3 is presented in Fig. S8a, All the reflections of Sb_2S_3 crystals obtained can be indexed to an orthorhombic phase of Sb_2S_3 (JCPDS Files, No.42-1393). Fig. S8b shows the SEM image of the as-prepared pure Sb_2S_3, which reveals a lot of nanorod.

The photocatalytic activity of $Sb_2S_3/Sb_4O_5Cl_2$ and pure Sb_2S_3 are carried out by degradation of methyl orange (MO) under visible light irradiation ($\lambda \geq 400$ nm). As

shown in Fig. S9, the degradation efficiency of the C1, C2, C3 and pure Sb_2S_3 are 63.5%, 84.3 %, 54.2% and 23.7 % after 60 min. The results indicate that $Sb_2S_3/Sb_4O_5Cl_2$ composites have higher catalytic activity than pure Sb_2S_3 under visible light. The enhanced optical absorption and suitable band gap are considered as significant factors for the improved catalytic activity. As shown in Fig. S10a, with the introduction of $Sb_4O_5Cl_2$, the optical absorption was obviously enhanced. The band gap was increased from 1.58eV to 2.45 eV, which was suitable for the improved catalytic activity. Additionally, comparing the morphology of pure Sb_2S_3 with $Sb_2S_3/Sb_4O_5Cl_2$ composite, the spherical structure, which is formed on the base of the three-dimensional framework of $Sb_4O_5Cl_2$, may be another important factor to affect the photocatalytic performance.

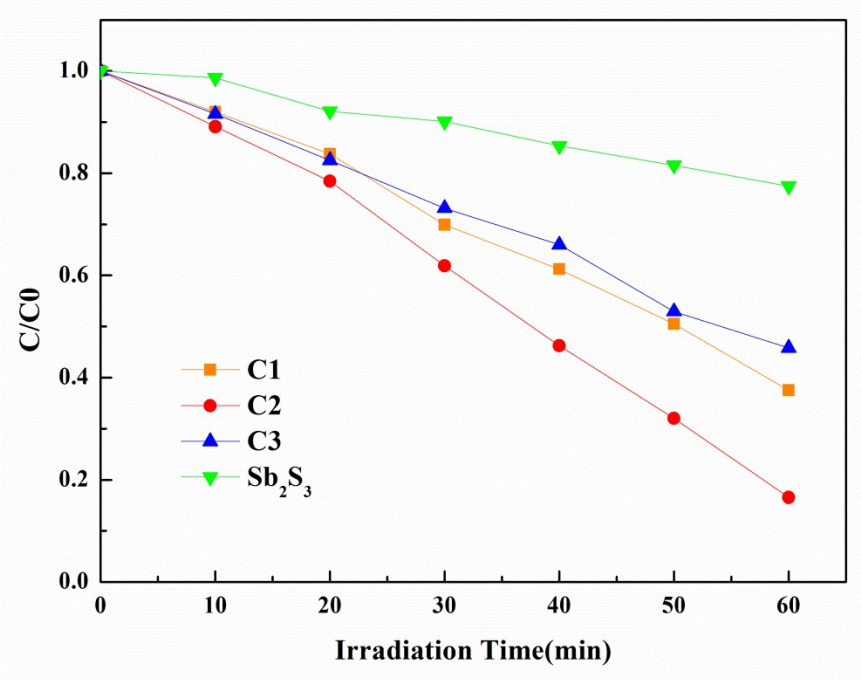

Fig. S9. Photocatalytic degradation of MO over different samples under visible light (λ≥420 nm) irradiation.

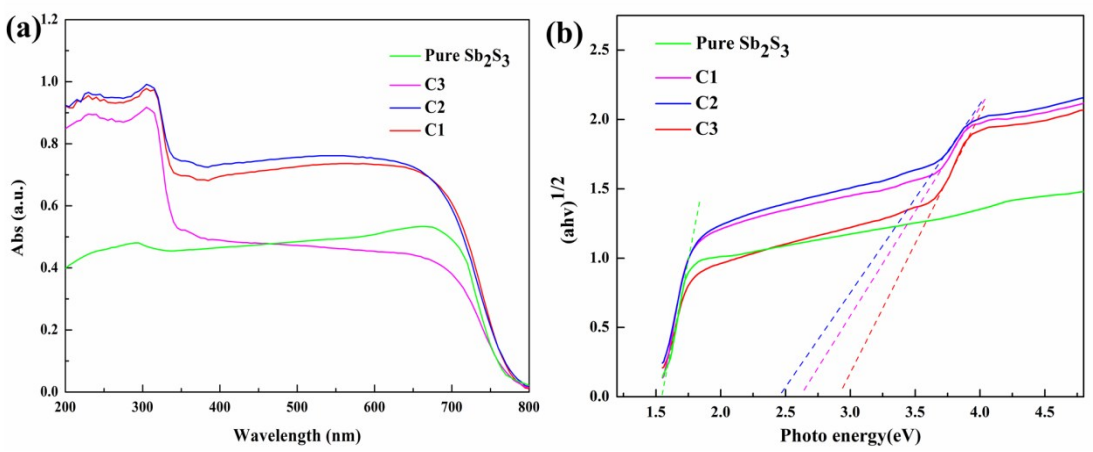

Fig. S10. (a) UV–vis diffuse reflectance spectra of different samples; (b) the band gaps (Eg) of different samples.